ANALYSES OF MOLECULAR STRUCTURE, VIBRATIONAL SPECTRA, NBO, HOMO-LUMO AND NLO STUDIES OF 1,5-DIFLUORO-2,4-DINITROBENZENE AND 1-CHLORO-2,4-DINITROBENZENE

Anitha Rexalin Devaraj[1, a], J.Geethapriya[2, b] , M.Arivazhagan[3, c]
[1] Department of Physics, Academy of Maritime Education and Training (AMET) University,135, East Coast Road, Kanathur - 603112, India.
[2] P.G & Research Department of Physics, National College, Trichy- 620 001, Tamil Nadu, India.
[3] Department of Physics, Government Arts College, Thiruverumbur- 620 022, Tamil Nadu, India.

ABSTRACT

Benzene is a clear, colorless, non-corrosive and highly flammable liquid with a sweet odour. Benzene is mostly widely-produced derivatives include styrene, which is used to make polymers and plastics. Benzene is also used to make some types of rubbers, lubricants, dyes, detergents, drugs and pesticides. Interestingly, dinitrobenzene belongs to the group of organic halogen compounds and used in the fumigant and insecticide, solvent, chemical intermediate to manufacture dyes, agrochemical, pharmaceuticals and other organic synthesis. As a continuation of the recent studies on structural and theoretical investigations of some substituted benzene derivatives, the main aspects of this investigation are: Structural analysis, molecular geometries and vibrational spectra of 1,5-difluoro-2,4-dinitrobenzene (DFDNB) and 1-chloro-2,4-dinitrobenzene (CDNB) are calculated by applying density functional theory (DFT) and *ab initio* (HF) computations and HOMO–LUMO, NBO analyses have been used to give more information regarding charge transfer within the molecules.

Keywords: DFT; NBO; HOMO-LUMO; FT-IR; FT-Raman

1. INTRODUCTION

Benzene is a clear, colorless, non-corrosive and highly flammable liquid with a sweet odour. It evaporates into the air very quickly and dissolves slightly in water [1]. Benzene is mainly used as an intermediate to make other chemicals; its mostly widely-produced derivatives include styrene, which is used to make polymers and plastics [2]. Benzene is also used to make some types of rubbers, lubricants, dyes, detergents, drugs and pesticides. Natural sources of benzene include volcanoes and forest fires. Benzene is

also a natural part of crude oil, gasoline and cigarette smoke [3-5]. At one time, chlorobenzene is the main precursor for the manufacture of phenol. The major use of chlorobenzene is an intermediate in the production of commodities such as herbicides, dyestuffs, and rubber. Chlorobenzene is also used as high-boiling solvent in many industrial applications as well as in the laboratory [6]. Interestingly, dinitrobenzene belongs to the group of organic halogen compounds and used in the fumigant and insecticide, solvent, chemical intermediate to manufacture dyes, agrochemical, pharmaceuticals and other organic synthesis.

As a continuation of the recent studies on structural and theoretical investigations of some substituted benzene derivatives, the main aspects of this investigation are: Structural analysis, molecular geometries and vibrational spectra of 1,5-difluoro-2,4-dinitrobenzene (DFDNB) and 1-chloro-2,4-dinitrobenzene (CDNB) are calculated by applying density functional theory (DFT) and *ab initio* (HF) computations and HOMO–LUMO, NBO analyses have been used to give more information regarding charge transfer within the molecules.

2. EXPERIMENTAL DETAILS

The samples of 1,5-difluoro-2,4-dinitrobenzene and 1-chloro-2,4-dinitrobenzene are purchased from Sigma Aldrich Chemicals, U.S.A. and used as such for recording spectra without further purification. The FT-IR spectra of DFDNB and CDNB compounds were recorded using BRUKER IFS 66V spectrometer in the region 4000–400 cm^{-1} with the spectral resolutions of ± 2 cm^{-1}. The FT-Raman spectra of DFDNB and CDNB were also recorded in the same instrument with FRA 106 Raman module equipped with Nd:YAG laser as source operating at 200 mW power with excitation frequency at 1064 nm line. The spectra were recorded in the region 3500–50 cm^{-1} with scanning speed of 30 cm^{-1} min^{-1} of spectral width 2 cm^{-1}. The frequencies of all sharp bands are accurate to ± 1 cm^{-1}.

3. COMPUTATIONAL DETAILS

For meeting, the requirements of both, accuracy and computing economy, theoretical methods and basis set should be considered. The *ab initio* and DFT calculations are carried out for DFDNB and CDNB with GAUSSIAN 09W program package [7]. Initial geometry generated from the standard geometrical

parameters is minimized without any constraint on the potential energy surface by employing the Becke 3LYP keyword which invokes Becke's three parameter hybrid method [8] using the correlation function of Lee et al. [9]. This geometry is then optimized again at B3LYP/6-311++G(d,p) for better description of bonding properties of the molecules. All the parameters are allowed to relax, and all the calculations converged to an optimized geometry which corresponds to a true minimum, as revealed by the lack of imaginary values in the wavenumber calculations. The Cartesian representation of theoretical force constants have been computed at the fully optimized geometry. The multiple scaling of force constants is performed according to SQM procedure [10,11] using selective scaling in natural internal co-ordinate representation. Transformation of force field, the subsequent normal co-ordinate analysis including the least square refinement of the scale factors and calculation of total energy distribution calculation are done on a PC with the MOLVIB program (version V 7.0 – G77) written by Sundius [12-14]. The systematic comparison of the results from DFT theory with results of experiments has shown that the method using B3LYP/6-311++G(d,p) functional is the most promising in providing correct vibrational wavenumbers. The bond length and bond angles of DFDNB and CDNB are given in Tables 1 and 2, respectively. Normal coordinate analysis is carried out for DFDNB and CDNB to provide a complete vibrational assignment of fundamental frequencies. For this purpose, the full set of 54 standard internal coordinates (containing 12 redundancies) for both DFDNB and CDNB are defined and given in Tables 3 and 4, respectively. From these, a non-redundant set of local symmetry coordinates are constructed by suitable linear combinations of internal coordinates following the recommendations of Fogarasi *et al.* [15] and are summarized in Tables 5 and 6. The theoretically calculated force fields are transformed to this set of vibrational coordinates and used in all subsequent calculations.

3.1. Prediction of Raman Intensities

The Raman activities are subsequently converted to relative Raman intensities (I_i) using the following relationship derived from the basic theory of Raman scattering [1,2,16]:

$$I_i = \frac{f(\nu_o - \nu_i)^4 S_i}{n_i \left[1 - \exp\left(-\frac{hc\nu_i}{kT}\right)\right]} \quad \text{... (1)}$$

where, ν_0 is the laser exciting wavenumber in cm^{-1} (in this, the used excitation wavenumber ν_0 = 9398.5 cm^{-1}, which corresponds to the wavelength of 1064 nm of a Nd:YAG laser), ν_i is the vibrational wavenumber of the i^{th} normal mode (cm^{-1}), while S_i is the Raman scattering activity of the normal mode ν_i, f (is a constant equal to 10^{-12}) is a suitably chosen common normalization factor for all peak intensities. h, k, c and T are Planck and Boltzmann constants, speed of light and temperature in Kelvin, respectively.

4. RESULTS AND DISCUSSION

4.1. Molecular Geometry

Molecular structure along with numbering of atoms of DFDNB and CDNB are shown in Figs 1 and 2, respectively. The maximum number of potentially active observable fundamentals of a non-linear molecule which contains N atoms is equal to (3N – 6), apart from three translational and three rotational degrees of freedom. Both DFDNB and CDNB consists of 16 atoms, hence they undergo 42 normal modes of vibrations. The molecules are considered under C_1 point group symmetry. The symmetry of the molecules is also helpful in making vibrational assignment. To check whether the chosen set of symmetric coordinates contribute maximum to the potential energy associated with the compound, the TED has been carried out. The vibrational problem is set-up in terms of internal and symmetry coordinates. The FT-IR and FT-Raman spectrum of DFDNB and CDNB are shown in Figs. 3-6.

4.2. Vibrational frequency analysis

The goal of the vibrational analysis is to find vibrational modes connected with molecular structures of investigated compounds. The numerical harmonic vibrational analysis for DFDNB and CDNB is done for the optimized geometry. The absence of negative frequencies for the stationary points found at the molecular potential energy hyper surfaces confirming that this structure corresponds to real minimum. Vibrational spectral assignments are performed on the recorded FT-IR and FT-Raman spectra based on theoretically predicted wavenumbers and their TED. The observed and calculated wavenumbers along with their relative intensities, scattering activities and probable assignments with TED of DFDNB and CDNB compounds are given in Tables 7 and 8, respectively. It should be noted that the calculations are made for a free molecule in vacuum, while the experiment is performed for the solid sample. Furthermore, the

anharmonicity is neglected in the real system for the calculated vibrations. Therefore, there are disagreements between the calculated and observed vibrational wavenumbers and because of the low IR intensities of some modes, it is difficult to observe them in the IR spectrum. In order to improve the agreement of theoretically calculated frequencies with experimentally calculated frequencies, it is necessary to scale down the theoretically calculated harmonic frequencies. Hence, the theoretically calculated vibrational frequencies at HF/6-311++G(d,p), B3LYP/6-311++G(d,p) methods are scaled by using MOLVIB 7.0 version written by Tom Sundius [14,17].

C–H vibrations

The nitro group does not appear to affect the position of characteristic C–H bands and these bands occur in the range 3100–3000 cm^{-1}. The in-plane C–H bending vibrations appear in the range 1300–1000 cm^{-1} in the substituted benzenes and the out-of-plane bending vibrations in the range 1000–750 cm^{-1} [18]. The FT-IR vibrational frequencies observed at 3139, 3128 and 3108, 3096, 3027 cm^{-1} are assigned to C–H stretching vibrations of DFDNB and CDNB respectively and show good agreement with the calculated results. The Raman counterpart of C–H vibration is observed at 3098 cm^{-1}, which are further supported by the TED contribution of almost 100%. The FT-Raman bands at 1160, 1144 and 1100 cm^{-1} and infrared bands at 1157, 1140 and 1103 cm^{-1} are assigned to C–H in-plane bending vibrations of CDNB. Accordingly, the FT-Raman band observed at 1545 cm^{-1} and infrared bands at 1578, 1546 cm^{-1} are assigned to C–H in-plane bending vibrations of DFDNB. The observed C–H out-of-plane bending modes of DFDNB and CDNB compounds show consistent agreement with the computed HF and B3LYP results and are listed in Tables 7 and 8, respectively.

C–C vibrations

The C–C aromatic stretching vibrations gives rise to characteristic bands in both the observed IR and Raman spectra, covering the spectral range from 1600 to 1400 cm^{-1} [19,20]. Therefore, the C–C stretching vibrations of CDNB are found at 1612, 1600, 1467 and 1298 cm^{-1} in FT-IR and 1478, 1392, 1300 cm^{-1} in the FT-Raman spectra. Further, the C–C stretching vibrations of the DFDNB are found at 1630, 1615, 1482 cm^{-1} and 1665, 1659, 1610, 1470 cm^{-1} in the FT-IR and FT-Raman spectra, respectively. These modes are

confirmed by their TED values. Most of the ring vibrational modes are affected by the substitutions in the aromatic ring of DFDNB and CDNB. In the present investigation, the bands observed at 1048, 916, 903 cm^{-1} in FT-IR and 1045, 915, 900 cm^{-1} in Raman spectra have been designated to ring in-plane bending modes of CDNB. The ring out-of-plane bending modes of CDNB are also listed in the Table 8. Further, the ring in-plane and out-of-plane bending vibrations are made for DFDNB by careful consideration of their qualitative descriptions and are reported in Table 7. The reductions in the frequencies of these modes are due to the change in force constant and the vibrations of the functional groups present in the molecules. The theoretically computed values for C–C vibrational modes of the compounds by B3LYP/6-311++G(d,p) method gives excellent agreement with experimental data.

C–N vibrations

In aromatic compounds, the C–N stretching vibrations usually lie in the region 1400–1200 cm^{-1}. The identification of C–N stretching frequencies is a rather difficult task, since the mixing of vibrations is possible in this region [21,22]. In the present investigation, the bands observed at 1242 cm^{-1} in IR and 1255 cm^{-1} in Raman spectra have been assigned to C–N stretching vibrations of CDNB. The FT-IR band appeared at 1428 and 1416 cm^{-1} has been designated to C–N stretching vibrations of DFDNB. The C–N in-plane and out-of-plane bending vibrations are also been identified and presented in Tables 7 and 8, respectively for DFDNB and CDNB. These assignments are also supported by the TED values.

NO_2 group vibrations

The characteristic group frequencies of the nitro group are relatively independent of the rest of the molecule which makes this group convenient to identify. Aromatic nitro compounds have strong absorptions due to the asymmetric and symmetric stretching vibrations of the NO_2 group at 1570–1485 cm^{-1} and 1370–1320 cm^{-1}, respectively [23]. Hence, the asymmetric stretching mode of nitro group for CDNB is identified at 1593, 1538 and 1535 cm^{-1} in FT-IR and FT-Raman spectra, respectively and in good agreement with TED output. The symmetric stretching mode of nitro group is assigned at 1350 cm^{-1} in IR and 1362 cm^{-1} in Raman spectra for CDNB. For DFDNB, the asymmetric stretching mode of nitro group is identified at 1533 cm^{-1} in IR, 1513 cm^{-1} in Raman spectrum and they are in good agreement with TED output. The

bands found at 1350 and 1321 cm^{-1} in IR spectrum has been designated to NO_2 symmetric stretching mode of DFDNB. The NO_2 scissoring mode for CDNB has been designated to the bands at 734 and 742 cm^{-1} in IR and Raman spectra, respectively. The scissoring modes of NO_2 group for DFDNB has been designated to the peak at 915 cm^{-1} in IR and 962, 910 cm^{-1} in Raman spectrum. The deformation vibrations of NO_2 group (rocking, wagging and twisting) contribute to several normal modes in the low frequency region [24]. These bands are also found well within the characteristic region and summarized in Tables 7 and 8, respectively for DFDNB and CDNB.

C–Cl vibrations

The vibrations belong to the bond between the ring and the halogen atoms are worth to discuss here, since mixing of vibrations are possible due to the lowering of the molecular symmetry and the presence of heavy atoms on the periphery of molecule [25]. Generally, the C–Cl absorption is obtained in the broad region between 850 and 550 cm^{-1} [26]. For CDNB, the bands found at 749 and 750 cm^{-1} in the FT-IR and FT-Raman spectrum have been designated to C–Cl stretching mode of vibration and the corresponding force constant contribute 72% to the TED. Most of the aromatic chloro compounds have the band of strong to medium intensity in the region 385–265 cm^{-1} due to C–Cl in-plane bending vibration Accordingly, the band identified at 372 cm^{-1} in Raman are assigned to the C–Cl in–plane mode of CDNB. The C–Cl out-of-plane deformation for CDNB has been established at 214 cm^{-1} in the Raman spectrum. These are in good agreement with the literature data [27].

C–F vibrations

In the vibrational spectra of related compounds, the bands due to C–F stretching vibrations [28] may be found over a wide frequency range 1360–1000 cm^{-1}, since the vibration is easily affected by adjacent atoms or groups. In the present investigation, the FT-IR band observed at 1303 cm^{-1} and Raman band observed at 1275 cm^{-1} have been assigned to C–F stretching mode of vibration for DFDNB. The corresponding in plane and out-of-plane bending vibrations have been identified and reported in Table 7.

5. FIRST HYPERPOLARIZABILITY

The potential application of DFDNB and CDNB molecules in the field of non-linear optics demands the investigation of its structural and bonding features contributing to the hyperpolarizability enhancement, by analyzing the vibrational modes using IR and Raman spectroscopy. The first hyperpolarizability (β) of this novel molecular system of DFDNB and CDNB are calculated using the DFT quantum mechanical method, based on the finite field approach. In the presence of an applied electric field, the energy of a system is a function of the electric field. The first hyperpolarizability is the third-rank tensor that can be described by a 3 × 3 × 3 matrix. The 27 components of the 3D matrix can be reduced to 10 components due to Klienman symmetry [29].

The components of β are defined as the coefficients in the Taylor series expansion of the energy in the external electric field. When the electric field is weak and homogeneous, this expansion becomes,

$$E = E_0 - \sum_i \mu_i F^i - \frac{1}{2}\sum_{ij} \alpha_{ij} F^i F^j - \frac{1}{6}\sum_{ijk} \beta_{ijk} F^i F^j F^k - \frac{1}{24}\sum_{ijkl} \gamma_{ijkl} F^i F^j F^k F^l + ... \quad ... (2)$$

where E_0 is the energy of the unperturbed molecule. F^i is the field at the origin and μ_i, α_{ij}, β_{ijk} and ν_{ijkl} are the components of dipole moment, polarizability, the first hyper polarizability and second hyperpolarizabilities, respectively. The calculated total dipole moment (μ) and mean first hyperpolarizability (β) of the CDNB molecule are 4.2227 Debye and 1.398 × 10^{-30} esu and for DFDNB molecule are 3.1460 Debye and 4.7869 × 10^{-30} esu, respectively. When compared these values with the value of urea, CDNB molecule is 4.7 times greater than urea and DFDNB molecule is 6.5 times greater than urea. The non-linear optical properties of DFDNB and CDNB are listed in Table 9. The large value of hyperpolarizability β, which is a measure of the non-linear optical activity of the molecular system is associated with the intramolecular charge transfer, resulting from the electron cloud movement through π conjugated frame work from electron donar to electron acceptor groups. The physical properties of these conjugated molecules are governed by the high degree of electronic charge delocalization along the charge transfer axis and by the low band gaps. So the title molecules are an attractive object for future studies of non linear optical properties.

6. HOMO–LUMO ANALYSIS

The interaction of two atomic (or) molecular orbitals produces two new orbitals. One of the new orbitals is higher in energy than original ones (the antibonding orbital) and one is lower (the bonding orbital). When one of the initial orbitals is filled with a pair of electrons (a Lewis base) and the other is empty (a Lewis acid). The "filled-empty" interaction therefore is stabilizing. Dealing with the interacting molecular orbitals, the two that interact are generally the highest energy occupied molecular orbital (HOMO) of one molecule, the lowest energy unoccupied molecular orbital (LUMO) of the other molecule. These orbitals are the pair that lies closest in energy of any pair of orbitals in two molecules, which allows them to interact more strongly. These orbitals are sometimes called the frontier orbitals, because they lie at the outer most boundaries of the electrons of the molecules.

The HOMO (highest occupied molecular orbital) - LUMO (lowest unoccupied molecular orbital) energy gap of DFDNB and CDNB have been calculated at the B3LYP/6-311++G(d,p). Many organic molecules containing conjugated π electrons are characterized hyperpolarizabilities are analyzed by means of vibrational spectroscopy [30,31]. In most cases, even in the absence of inversion symmetry, the strongest bands in the Raman Spectrum are weak in the IR spectrum and vice versa. But the intramolecular charge transfer from the donor to acceptor group through a single-double bond conjugate path can include large variations of both molecular dipole moments and molecular polarizability making IR and Raman activity at the same time. The experimental spectroscopic behaviour described above is well accounted for DFT calculations in π-conjugated systems that predict exceptionally large Raman and infrared intensities in IR and Raman spectra are comparable resulting from the electron cloud movement through π-conjugated frame work electron donor to electron acceptor groups. The analysis of wave function indicates that the electron absorption corresponds to the transition from the ground to first excited stated and is mainly described by one electron excitation from the HOMO to LUMO. The atomic orbital compositions of the frontier molecular orbital and few MOS for DFDNB and CDNB are sketched in Figs. 7 and 8, respectively.

The energy gap reflects the chemical activity of the molecules. LUMO as electron acceptor represents the ability to obtain an electron, HOMO represent the ability to donate the electron. Moreover,

the lower in HOMO–LUMO energy gap explains the eventual charge transfer interactions taking place within the molecules, which influences the biological activity of the molecule.

6.1. HOMO–LUMO energy gap and related molecular properties

The energy gap of DFDNB and CDNB is calculated at B3LYP/6-311++G(d,p) basis set level. Associated within the framework of SCF MO theory, the ionization energy and electron affinity can be expressed through HOMO and LUMO orbital energies as $I = -E_{HOMO}$ and $A = -E_{LUMO}$. The hardness corresponds to the gap between the HOMO and LUMO orbital energies. The larger the HOMO–LUMO energy gaps the harder the molecule [32]. The global hardness, $\eta = \frac{1}{2}(E_{LUMO} - E_{HOMO})$. The hardness has been associated with the stability of chemical system. The electron affinity can be used in combination with ionization energy to give electronic chemical potential, $\mu = \frac{1}{2}(E_{HOMO} + E_{LUMO})$. The global electrophilicity index, $\omega = \frac{\mu^2}{2\eta}$ is also calculated and listed in Table 10 for DFDNB and CDNB.

7. NBO ANALYSIS

The interactions between the orbitals can be interpreted through NBO theory. NBO theory allows the assignment of the hybridization of atomic lone pairs and of the atoms involved in bond orbitals. These are important data in spectral interpretation since the frequency ordering is related to the bond hybrid composition [33].

The natural bond orbital analyses provide an efficient method for studying intra and inter molecular bonding and interaction among bonds and also provides a convenient basis for investigating charge transfer (or) conjugative interaction in molecular systems. Some electron donor orbital, acceptor orbital and the interacting stabilization energy resulting from the second-order micro disturbance theory reported [34,35]. The result of interaction is a loss of occupancy from the concentration of electron NBO of the idealized Lewis structure in to an empty non-Lewis orbital. For each donor (i) and acceptor (j), the stabilization energy E(2) associated with delocalization $i \rightarrow j$ is estimated as,

$$E(2) = -n_\sigma \frac{\langle \sigma | F | \sigma \rangle^2}{\varepsilon_\sigma^* - \varepsilon_\sigma} = -n_\sigma \frac{F_{ij}^2}{\Delta E} \qquad \ldots (3)$$

where $\langle\sigma|F|\sigma\rangle^2$ (or) F_{ij}^2 is the Fock matrix element i and j NBO orbitals, ε_σ and ε_σ^* are the energies of σ and σ* NBO's and n_σ is the population of the donar σ orbital.

Larger the E(2) value, the interaction between electron donors and electron acceptors is more intensive and greater the extent of conjugation of whole system. The intra-molecular hyperconjugative interactions are formed by the orbital overlap between π (C–C) and geminal π*(C–C) bond orbitals which results in intra-molecular charge transfer (ICT) causing stabilization of the system are presented in Tables 11 and 12, respectively for DFDNB and CDNB. In DFDNB the electron donating from n(3) O10 to the π* (N8–O9) and from n(3) O14to the π* (N12–O13) show high enormous stabilization energy of 339.677and 372.125 kJ/mol. In CDNB the interaction between, donar π*(C_1–C_6) and acceptor π*(C_2–C_3) and the interaction between, donar π*(C_1–C_6) and acceptor π*(C_4–C_5) shows high enormous stabilization energy of 232.11and 247.93 kJ/mol.

8. OTHER MOLECULAR PROPERTIES

The thermodynamic parameters namely heat capacity, entropy, rotational constants, dipole moments and zero-point vibrational energies (ZPVE) of DFDNB and CDNB have also been computed at DFT/B3LYP level using 6-311++G(d,p) as basis set and are presented in Table 13. The total energy and the change in the total entropy of the molecule at room temperature are also presented.

9. MULLIKEN CHARGE ANALYSIS

Mulliken atomic charge calculation has an important role in the application of quantum chemical calculations to molecular system because of atomic charges affect dipole moment, molecular polarizability, electronic structure and more a lot of properties of molecular systems. The charge distributions calculated by the Mulliken [36] for the equilibrium geometry of DFDNB and CDNB are listed in Tables 14 and corresponding Mulliken's plots are shown in Figs. 9 and 10, respectively. The atomic charge obtained from B3LYP/6-311++G(d,p) shows that the natural atomic charges are more sensitive to the changes in the molecular structure than Mulliken's net charges.

10. CONCLUSION

The molecular structural parameters, thermodynamic properties and vibrational frequencies of the fundamental modes of the optimized geometry of 1,5-difluoro-2,4-dinitrobenzene and 1-chloro-2,4-dinitrobenzene have been determined from *ab initio* and DFT calculations. The theoretical results are compared with the experimental values. The detailed reliable vibrational assignments and analysis of the molecules are carried out. The effects of substituents fluoro, chloro and nitro group moiety on the vibrational frequencies bonding in DFDNB and CDNB influence the structural parameters are discussed. The deviation between the experimental and calculated frequencies are reduced with use of HF/6-311++G(d,p) and B3LYP/6-311++G(d,p) levels of calculations and B3LYP/6-311++G(d,p) is considered as more reliable method. NLO property has also observed by predicting the first hyperpolarizability for DFDNB and CDNB molecules due to the substitution in the benzene. NBO study reveals that lone pair orbital participates in electron donation to stabilize the molecules. Natural bond orbital analysis of the molecule confirms that the intramolecular charge transfer caused by π-electron cloud movement from donor to acceptor must be responsible for the non-linear optical properties of DFDNB and CDNB. The results will help researchers to design and synthesis of new materials. Decrease in HOMO and LUMO energy gap explains the eventual charge transfer occurs within the molecules which is responsible for the chemical reactivity of the molecules. These calculations are carried out in ground state by using density functional theory.

REFERENCES

[1] G. Keresztury, S. Holly, J. Varga, G. Besenyei, A.Y. Wang, J.R. Durig, Spectrochim. Acta Part A, **49** (1993) 2007.

[2] P.L. Polavarapu, J. Phys. Chem., **94** (1990) 8106.

[3] G. Keresztury, Raman Spectroscopy: Theory in: J.M. Chalmers, P.R. Griffiths (Ed.), Handbook of Vibrational Spectroscopy, Wiley, **1** (2002).

[4] J. Choo, S. Kim, H. Joo, Y. Know, J. Mol. Struct., **587** (2002) 1-8.

[5] S. George, Infrared and Raman Characteristic Group frequencies, Tables and Charts, third ed., Wiley, Chichester, 2001.

[6] H. Susi, J.S. Ard, Spectrochim. Acta A **27** (1971) 1549-1562.

[7] M.J. Frisch, G.W. Trucks, H.B. Schlegal, G.E. Scuseria, M.A. Robb, J.R. Cheesman, G. Zakrzewski, J.A. Montgomerg, Jr., R.E. Stratmann, J.C. Burant, S. Dapprich, J.M. illam, A.D. Daniels, K.N. Kudin, M.C. Strain, O. Farkas, J. Tomasi, V. Barone, M. Cossi, R. Cammi, B. Mennucci, C. Pomelli, C. Adamo, S. Clifford, J. Ochterski, G.A. Petersson, P.Y. Ayala, Q. Cui, K. Morokuma, N. Rega, P. Salvador, J.J. Dannenberg, D.K. Malich, A.D. Rabuck, K. Raghavachari, J.B. Foresman, J. Cioslowski, J.V. Ortiz, A.G. Baboul, B.B. Stetanov, G. Liu, A. Liashenko, P. Piskorz, I. Komaromi, R. Gomperts, R.L. Martin, D.J. Fox, T. Keith, M.A. Al-Laham, C.Y. Peng, A. Nanayakkara, M. Challacombe, P.M.W. Gill, B. Johnson, W. Chen, M.W. Wong, J.L. Andres, C. Gonzalez, M. Head-Gordon, E.S. Replogle, J.A. Pople, GAUSSIAN 09, Revision A 11.4, Gaussian, Inc., Pittsburgh PA, 2009.

[8] C. Lee, W. Yang, R.G. Parr, Phys. Rev., **B37** (1988) 785.

[9] A.D. Becke, Journal of Chemical Physics, **98** (1993) 5648.

[10] P. Pulay, G. Fogarasi, G. Pongor, J.E. Boggs, A. Vargha, Journal Am. Chem. Soc. **105** (1983)7037.

[11] G. Rauhut, P. Pulay, J. Phys. Chem., **99** (1995) 3093.

[12] T. Sundius, Journal of Molecular Structure, **218** (1990) 321.

[13] MOLVIB (V.7.0): Calculation of Hormonic Force Fields and Vibrational Modes of Molecules, QCPE program No. 807 (2002).

[14] T. Sundius, Vibrational Spectroscopy, **29** (2002) 89.

[15] G. Fogarai, X. Zhou, P.W. Taylor, P. Pulay, J. Am. Chem. Soc. **114** (1992) 8191.

[16] R.M. Silverstein, G. Clayton Basseler, Morrill, Spectrometric identification of Organic Compounds, John Wiley and Sons, New York, 1991.

[17] T. Sundius, Journal of Molecular Spectroscopy, **82** (1980) 138.

[18] V. Krishnakumar, N. Prabavathi, Spectrochimica, Acta **72A** (2009) 738-742.

[19] G. Socrates, IR and Raman Characteristics Group Frequencies Tables and Charts, 3rd ed., Wiley, Chichester (2001) 107-111.

[20] S. Jeyavijayan, M. Arivazhagan, Spectrochim. Acta **81A** (2011) 466.

[21] D.N. Sathyanarayana, Vibrational Spectroscopy - Theory and Applications, second ed., New Age International (P) Limited Publishers, New Delhi, 2004.

[22] V. Krishnakumar, V. Balachandran, Spectrochim. Acta **61A** (2005) 1001.

[23] N. Sundaraganesan, S. Ayyappan, H. Umamaheswari, B. Dominic Joshua, Spectrochim., Acta **66A** (2007) 17.

[24] A. Kovacs, G. Keresztury, V. Izvekov, Chem. Phys., **253** (2000) 193.

[25] R.A. Yadav, I.S. Sing, Indian J. Pure Appl. Phys., **23** (1985) 626.

[26] V. Arjunan, S. Mohan, J. Mol. Struct., **892** (2008) 289.

[27] N. Sundaraganesan, B. Anand, B. Dominic Joshua, Spectrochim., Acta **65A** (2006) 1053-1062.

[28] D. Sajan, J. Binoy, I .Hubert Joe, V.S. Jayakumar Zaleski, J. Raman Spectrosc., **36** (2005) 221.

[29] D.A. Kleinman, Phys. Rev., **126** (1962) 1977.

[30] T. Vijayakumar, Hubert. Joe, C.P.R. Nair, V.S. Jayakumar, Chem. Phys., **343** (2008) 83.

[31] Y. Atalay, D. Avil, A. Basaoglu, Struct. Chem., **19** (2008) 239.

[32] D.F.V. Lewis, C. Ioannides, D.V. Parke, Xenobiotica, **24** (1994) 401.

[33] R.G. Pearson, J.Am. Chem. Soc., **107** (1985) 6801.

[34] L. Jun-na, C. Zhi-Rang, Y. Shen-Fang, J. Zhejiang, Univ. Sci., **68** (2005) 584.

[35] E.D. Glendening, J.K. Badenhoop, A.I. Reed, J.E. Carpenter, J.A. Bohmann, C.M. Morales, F. Weinhold, NBO S.O, Theoretical Chemistry Institute, University of Wisconsin, Madison 2001.

[36] C. James, A. Amal Raj, R. Reghunathan, I. Hubert Jue, V.S. Jayakumar, J. Raman Spectroscopy, **37** (2006) 1381.

Table 1: Optimized geometrical parameters of 1,5-difluoro-2,4-dinitrobenzene obtained by HF/6-311++G(d,p) and B3LYP/6-311++G(d,p) level calculations.

Bond Length	Value (Å)		Bond Angle	Value (°)		Dihedral Angle	Value (°)	
	HF	B3LYP		HF	B3LYP		HF	B3LYP
C1-C2	1.3896	1.3994	C2-C1-C6	120.396	121.1915	C6-C1-C21C3	0.2533	0.0216
C1-C6	1.3766	1.3862	C2-C1-F7	121.969	121.2716	C6-C1-C2-N8	-179.2123	179.474
C1-F7	1.2975	1.3767	C6-C1-F7	117.605	117.4804	F7-C1-C2-C3	-177.7725	177.2193
C2-C3	1.3779	1.3911	C1-C2-C3	119.65	119.4491	F7-C1-C2-N8	2.7619	-3.3283
C2-N8	1.4592	1.4625	C1-C2-N8	122.371	122.4494	C2-C1-C6-C5	1.0623	-1.4719
C3-C4	1.3779	1.3911	C3-C2-N8	117.975	118.0994	C2-C1-C6-H16	-178.5262	178.1242
C3-H11	1.0708	1.0793	C2-C3-C5	120.236	120.0397	F7-C1-C6-C5	179.1724	-178.7722
C4-C5	1.3896	1.3993	C2-C3-H11	119.867	119.9781	F7-C1-C6-H16	-0.4161	0.8239
C4-N12	1.4592	1.4625	C4-C3-H11	119.867	119.9804	C1-C2-C3-C4	-1.5815	1.4594
C5-C6	1.3766	1.3862	C3-C4-C5	119.651	119.4501	C1-C2-C3-H11	178.7397	-178.0524
C5-F15	1.2975	1.3767	C3-C4-N12	117.975	118.1009	N8-C2-C3-C4	177.9074	-178.0167
C6-H16	1.0725	1.0787	C5-C4-N12	122.371	122.4469	N8-C2-C3-H11	-1.7714	2.4715
N8-O9	1.1825	1.2618	C4-C5-C6	120.396	121.1915	C1-C2-N8-O9	22.8554	151.9183
N8-O10	1.1872	1.2668	C4-C5-F15	121.969	121.2689	C1-C2-N8-O10	-158.1343	-29.5223
N12-O13	1.1872	1.2668	C6-C5-F15	117.906	117.4832	C3-C2-N8-O9	-156.618	-28.6223
N12-O14	1.1825	1.2618	C1-C6-C5	119.613	118.6454	C3-C2-N8-O10	222.3915	149.9371
			C1-C6-H16	120.192	120.6764	C2-C3-C4-C5	1.5815	-1.4592
			C5-C6-H16	120.192	120.6769	C2-C3-C4-N12	-177.907	178.0195

			C2-N8-O9	117.621	118.2966	H11-C3-C4-C5	-178.739	178.0525
			C2-N8-O10	116.646	117.0604	H11-C3-C4-N12	1.7714	-2.4687
			O9-N8-O10	125.723	124.6258	C3-C4-C5-C6	-0.2533	-0.022
			C4-N12-O13	116.646	117.0597	C3-C4-C5-F15	177.7725	-177.2207
			C4-N12-O14	117.621	118.2954	N12-C4-C5-C6	179.2123	-179.4771
						C3-C4-N12-O13	-2.7619	-2.8619
						C3-C4-N12-O14	-22.8554	-21.8554
						C5-C4-N12-O13	156.618	156.678
						C5-C4-N12-O14	158.134	158.723
						C4-C5-C6-C1	-22.855	-22.9855
						C4-C5-C6-H16	-1.0623	-1.80623
						F15-C5-C6-C1	178.5262	178.262
						F15-C5-C6-H16	-179.172	-179.372

Table 2: Optimized geometrical parameters of 1-chloro-2,4–dinitrobenzene obtained by HF/6-311++G(d,p) and B3LYP/ 6-311++G(d,p) level calculations

Bond Length	Value (Å)		Bond Angle	Value (°)		Dihedral Angle	Value (°)	
	HF	B3LYP		HF	B3LYP		HF	B3LYP
C1-C2	1.4	1.3816	C2-C1-C6	118.5788	119.9631	C6-C1-C2-C3	-0.6418	-0.665
C1-C6	1.4045	1.38	C2-C1-Cl7	117.5515	124.0313	C6-C1-C2-H8	179.1606	179.2663
C1-Cl7	1.7291	1.7901	C6-C1-Cl7	123.8063	115.9849	Cl7-C1-C2-C3	-177.8569	177.6134
C2-C3	1.3861	1.3788	C1-C2-C3	121.0822	119.7707	Cl7-C1-C2-H8	1.9455	-2.4554
C2-N8	1.0824	1.4513	C1-C2-N8	118.6325	124.5064	C2-C1-C6-C4	-.5846	-0.2309
C3-C4	1.3918	1.3689	C3-C2-N8	120.2851	115.7228	C2-C1-C6-N14	178.8714	179.5786
C3-H11	1.0819	1.0652	C2-C3-H5	118.8197	119.5713	Cl7-C1-C6-C4	176.4437	-178.6437
C4-C5	1.3838	1.3771	C2-C3-C9	121.3007	119.7874	Cl7-C1-C6-N14	-4.1003	1.1658
C4-N12	1.3906	1.4463	C5-C3-H9	119.8776	120.6413	C1-C2-C3-C5	1.0383	1.1531
C5-C6	1.0815	1.3766	C5-C4-H6	118.8783	121.3853	C1-C2-C3-H9	-179.4814	-178.7796
C5-H15	1.4819	1.0672	C5-C4-C13	120.9978	119.117	H8-C2-C3-C5	-178.7609	-178.784
C6-H16	1.4847	1.0684	C6-C4-C13	120.1234	119.4974	H8-C2-C3-H9	.7194	1.2833
N8-O9	1.2219	1.2333	C3-C5-C4	121.7427	118.901	C2-C3-C5-C4	-22.04	-22.4396
N8-O10	1.2205	1.2488	C3-C5-N10	119.368	120.8807	C2-C3-C5-N10	157.0652	159.0652
N12-O13	1.2178	1.241	C4-C5-N10	118.8894	121.5934	H9-C3-C5-C4	158.4942	157.4942
N12-O14	1.2212	1.2429	C1-C6-C4	123.2344	120.3983	H9-C3-C5-N10	-21.001	-21.001
			C1-C6-N14	123.2344	119.0616	C6-C4-C5-C3	-.9735	-0.7625
			C4-C6-N14	115.8828	120.5397	C6-C4-C5-N10	179.0935	179.3956

			C5-C10-O11	117.0968	118.6589	H13-C4-C5-C3	179.2625	179.1696
			C5-C10-O12	117.4257	116.0115	H13-C4-C5-N10	-.6704	-0.6723
			C6-N14-O15	116.4119	125.3105	C5-C4-C6-C1	1.3744	-0.1281
			C6-N14-O16	125.734	117.2739	C5-C4-C6-N14	-178.1199	-179.833
						C3-C5-N10-O11	-178.8596	179.7133
						C3-C5-N10-O12	1.6462	0.0083
						C4-C5-N10-O11	-.8104	-0.4144
						C4-C5-N10-O12	-179.7022	179.6356
						C5-C4-N12-O13	179.1241	179.7407
						C5-C4-N12-O14	.2323	-0.2093
						C1-C6-N14-O15	-34.9523	-33.6251
						C1-C6-N14-O16	146.559	-148.1815
						C4-C6-N14-O15	144.5288	-142.1815
						C4-C6-N14-O16	-33.9599	-32.517

Table 3: Definition of standard internal co-ordinates of 1,5-difluoro- 2,4-dinitrobenzene.

No.	Symbol	Type	Definition[a]
Stretching			
1-6	R_i	C-C	C1-C2, C2-C3, C3-C4, C4-C5, C5-C6, C6-C1
7-8	r_i	C-H	C6-H16, C3-H12
9-10	s_i	C-F	C1-F7, C1-F15
11-12	Q_i	C-N	C2-N8, C4-N12
13-16	P_i	N-O	N8-O9, N8-O10, N12-O13, N12-O14
In-plane bending			
17-22	β_i	Ring	C1-C2-C3, C2-C3-C4, C3-C4-C5, C4-C5-C6, C5-C6-C1, C6-C1-C2
23-26	α_i	C-C-F	C2-C1-F7, C6-C1-F7, C4-C5-F6, C6-C5-F15
27-30	γ_i	C-C-H	C1-C6-H16, C5-C6-H16, C2-C3-H11, C4-C3-H11
31-34	∞_i	C-C-N	C3-C2-N8, C1-C2-N8, C3-C4-N12, C5-C4-N12
35-38	θ_i	C-N-O	C4-N3-O13, C4-N12-O14, C2-N8-O4, C2-N8-O10
39-40	θ_i	O-N-O	O13-N12-O14, O9-N8-O10
Out-of-plane bending			
41-42	ϕ	C-F	F7-C1-C2-C6, F15-C5-C4-C6
43-44	ϕ_i	C-H	H16-C6-C1-C5, H17-C3-C2-C4
45-46	λ_i	C-N	N8-C2-C1-C3, N12-C4-C3-C5
Torsion			
47-52	τ_i	τ ring	C1-C2-C3-C4, C2-C3-C4-C5, C3-C4-C5-C6, C4-C5-C6-C1, C5-C6-C1-C2, C6-C1-C2-C3
53-54	z_i	NO_2	C2-N8-O9-O10, C4-N12-O13-O14

[a] For numbering of atoms refer Fig. 1.

Table 4: Definition of standard internal co-ordinates of 1-chloro-2,4-dinitrobenzene

No.	Symbol	Type	Definition[b]
Stretching			
1-6	R_i	C-C	C1-C2, C2-C3, C3-C4, C4-C5,C5-C6, C6-C1
7-8	r_i	C-H	C6-H16, C3-H12
9	s_i	C-F	C1-F7, C1-F15
10-12	Q_i	C-N	C2-N8, C4-N12
13-16	P_i	N-O	N8-O9, N8-O10, N12-O13, N12-O14
In-plane bending			
17-22	β_i	Ring	C1-C2-C3, C3-C4-C5, C5-C6-C1
23-26	α_i	C-C-N	C1-C2-N8, C3-C2-N8, C3-C4-N12, C5-C4-N12
27-32	γ_i	C-C-H	C1-C6-H16, C5-C6-H16, C6-C5-H15, C4-C5-H15, C2-C3-H11, C4-C3-H11
33-34	φ_i	C-C-Cl	C6-C1-Cl7, C2-C1-Cl7
35-36	θ_i	C-N-O	O9-N8-O10, O13-N12-O14
37-40	θ_i	O-N-O	C2-N8-O9, C2-N8-O10, C4-N12-O13, C4-N12-O14
Out-of-plane bending			
41	w_i	C-Cl	Cl7-C1-C2-C6
42-44	ψ_i	C-H	H11-C3-C2-C4, H15-C5-C4-C6, H16-C6-C5-C1
45-46	π_i	C-N	N8-C2-C3-C1, N12-C4-C3-C5
Torsion			
47-52	τ_i	τ Ring	C1-C2-C3-C4, C2-C3-C4-C5,C3-C4-C5-C6, C4-C5-C6-C1, C5-C6-C1-C2, C6-C1-C2-C3
53-54	τ_i	τ_i-NO_2	C2-N8-O9-O10, C4-N12-O13-O14

[a] For numbering of atoms refer Fig. 2.

Table 5: Definition of local symmetry co-ordinates of 1,5-difluoro-2,4-dinitrobenzene

No.	Symbol[a]	Definition[b]
1-6	C-C	R_1, R_2, R_3, R_4, R_5, R_6
7-8	C-H	r_7, r_8
9-10	C-F	S_9, S_{10}
11-12	C-Cl	Q_{11}, Q_{12}
13-14	NO_2 ss	$(P_{13} + P_{14})/\sqrt{2}$, $(P_{15} + P_{16})/\sqrt{2}$
15-16	NO_2 ass	$(P_{13} + P_{14})/\sqrt{2}$, $(P_{15} + P_{16})/\sqrt{2}$
17	R trigd	$(\beta_{17} - \beta_{18} + \beta_{19} - \beta_{20} + \beta_{21} - \beta_{22})/\sqrt{6}$
18	R Symd	$(\beta_{17} - \beta_{18} + \beta_{19} - \beta_{20} + \beta_{21} - \beta_{22})/\sqrt{12}$
19	R asymd	$(\beta_{17} - \beta_{18} + \beta_{20} - \beta_{21})/\sqrt{2}$
20-21	bCF	$(\alpha_{23} - \alpha_{24})/\sqrt{2}$, $(\alpha_{25} - \alpha_{26})/\sqrt{2}$
22-23	bCH	$(\gamma_{27} - \gamma_{28})/\sqrt{2}$, $(\gamma_{29} - \gamma_{30})/\sqrt{2}$
24-25	bCN	$(\delta_{31} - \delta_{32})/\sqrt{2}$, $(\delta_{33} - \delta_{34})/\sqrt{2}$
26-27	NO_2rock	$(\theta_{35} - \theta_{36})/\sqrt{2}$, $(\theta_{37} - \theta_{38})/\sqrt{2}$
28-29	NO_2twist	$(\theta_{35} + \theta_{36})/\sqrt{2}$, $(\theta_{37} + \theta_{38})/\sqrt{2}$
30-31	NO_2sciss	$(2\theta_{39} - \theta_{35} - \theta_{36})/\sqrt{2}$, $(2\theta_{46} - \theta_{37} - \theta_{38})/\sqrt{2}$
32-33	WCF	ϕ_{41}, ϕ_{42}
34-35	WCH	φ_{43}, φ_{44}
36-37	WCN	λ_{45}, λ_{46}
38	tR trig	$(\tau_{47} - \tau_{48} + \tau_{49} - \tau_{50} + \tau_{51} - \tau_{52})/\sqrt{2}$
39	tR sym	$(\tau_{47} - \tau_{49} + \tau_{50} - \tau_{52})/\sqrt{2}$
40	tR assym	$(-\tau_{47} - 2\tau_{48} - \tau_{49} - \tau_{50} + \tau_{51} - \tau_{52})/\sqrt{2}$
41-42	NO_2wag	τ_{53}, τ_{54}

[a] These symbols are used for description of normal modes by TED.
[b] The internal co-ordinates used here are defined in Table 3.

Table 6: Definition of local symmetry co-ordinates of 1-chloro-2,4–dinitrobenzene

No.	Symbol[a]	Definition[b]
1-6	CC	$r_1, r_2, r_3, r_4, r_5, r_6$
7-8	CN	Q_7, Q_8
9	CCl	T_9
10-12	CH	R_{10}, R_{11}, R_{12}
13-14	NO_2 ss	$(P_{13} + P_{14})/\sqrt{2}$, $(P_{15} + P_{16})/\sqrt{2}$
15-16	NO_2ass	$(P_{13} - P_{14})/\sqrt{2}$, $(P_{15} - P_{16})/\sqrt{2}$
17	R trigd	$(\beta_{17} - \beta_{18} + \beta_{19} - \beta_{20} + \beta_{21} - \beta_{22})/\sqrt{6}$
18	R symd	$(-\beta_{17} - \beta_{18} + 2\beta_{19} - \beta_{20} - \beta_{21} + 2\beta_{22})/\sqrt{12}$
19	R asymd	$(\beta_{15} - \beta_{16} + \beta_{18} - \beta_{19})/\sqrt{2}$
20, 21	b CN	$(\alpha_{23} - \alpha_{24})/\sqrt{2}$, $(\alpha_{25} - \alpha_{26})/\sqrt{2}$
22-24	b CH	$(\gamma_{27} - \gamma_{28})/\sqrt{2}$, $(\gamma_{29} - \gamma_{30})/\sqrt{2}$, $(\gamma_{31} - \gamma_{32})/\sqrt{2}$
25	b Cl	$(\varphi_{33} - \varphi_{34})/\sqrt{2}$
26, 27	NO_2rock	$(\theta_{35} - \theta_{36})/\sqrt{2}$, $(\theta_{37} - \theta_{38})/\sqrt{2}$
28-29	NO_2twist	$(\theta_{35} - \theta_{36})/\sqrt{2}$, $(\theta_{37} - \theta_{38})/\sqrt{2}$
30-31	NO_2sciss	$(2\sigma_{39} - \sigma_{35} - \sigma_{36})/\sqrt{2}$, $(2\sigma_{40} - \sigma_{37} - \sigma_{38})/\sqrt{2}$
32	ω CCl	ω_{41}
33-35	Ψ CH	$\Psi_{42}, \Psi_{43}, \Psi_{44}$
36-37	π CO	π_{45}, π_{45}
38	τ R trigd	$(\tau_{47} - \tau_{48} + \tau_{49} - \tau_{50} - \tau_{51} - \tau_{52})/\sqrt{6}$
39	τ R symd	$(\tau_{47} - \tau_{49} + \tau_{50} - \tau_{52})/\sqrt{2}$
40	τ R asymd	$(-\tau_{47} + 2\tau_{48} - \tau_{49} - \tau_{50} + 2\tau_{51} - \tau_{52})/\sqrt{12}$
41-42	NO_2wag	τ_{53}, τ_{54}

[a] These symbols are used for description of normal modes by TED.
[b] The internal co-ordinates used here are defined in Table 4.

Table 7: The observed (FT-IR and FT-Raman) and calculated (Unscaled and Scaled) frequencies (cm^{-1}), IR intensity (Km mol^{-1}), Raman activity (A^4 amu^{-1}) and probable assignments (characterized by TED) of 1,5-difluoro-2,4-dinitrobenzene using HF/6-311++G(d,p) and B3LYP/6-311++G(d,p) calculations.

S. No.	Observed frequency (cm^{-1})		HF/6-311++G(d,p)						B3LYP/6-311++G(d,p)						Assignment % of TED
	FT-IR	FT-Raman	Calculated frequencies (cm^{-1})		Reduced Mass	Force Constants	IR Intensity	Raman Activity	Calculated frequencies (cm^{-1})		Reduced Mass	Force Constants	IR Intensity	Raman Activity	
			Unscaled	Scaled					Unscaled	Scaled					
1	3139	-	3334	3139	1.0947	7.1723	25.2472	42.7608	3234	3130	1.0937	6.7424	3.7021	125.355	νCH(99)
2	3128	-	3329	3135	1.0955	7.1573	20.5592	80.1034	3229	3127	1.0923	6.7143	27.7129	11.3753	νCH(98)
3	-	1665	1752	1674	6.4482	11.6695	205025	63.0252	1648	1669	7.2956	11.6730	174.436	71.2561	νCC(96)
4	-	1659	1703	1663	10.5200	18.5700	141.5238	22.5170	1626	1655	10.7360	16.7185	104.309	32.0503	νCC(96)
5	1630	-	1608	1641	3.0829	4.7011	83.0966	6.2419	1520	1635	3.4100	4.6406	66.0836	17.0135	νCC(89)
6	1615	1610	1514	1626	10.2751	13.8935	47.6574	29.3781	1480	1620	12.5757	16.2246	197.677	37.2019	νCC(92)
7	1578	-	1367	1589	12.2815	13.5268	142.1867	198.5099	1450	1583	11.1233	13.7815	50.0782	9.0239	bCH(86)
8	1546	1545	1349	1561	2.5415	2.7288	121.7293	15.9354	1400	1550	11.7073	13.5150	72.5321	2.9503	bCH(84)
9	1533	-	1344	1539	2.0825	2.2185	340.9106	16.3092	1366	1531	11.0850	12.1859	25.1901	1.4038	NO_2 ass(84)
10		1513	1272	1522	3.6495	3.4798	97.8476	0.9802	1289	1517	12.6175	12.3565	190.977	283.257	NO_2 ass(83)
11	1482	-	1268	1596	10.6836	10.1209	80.9149	8.7012	1277	1589	11.1746	10.7354	7.5746	8.8274	νCC(82)
12		1470	1191	1478	13.2094	11.0423	391.0412	8.5287	1271	1473	2.6904	2.5626	111.741	37.3733	νCC(80)
13	1428	1430	1161	1436	2.3718	1.8837	14.0804	0.3494	1263	1429	2.0816	1.9559	198.378	33.1606	νCN(78)
14	1416	1425	1157	1427	10.7462	8.4804	383.3010	3.3812	1165	1420	1.7348	1.3881	17.4840	2.4483	νCN(77)
15	1350	-	1148	1352	11.0331	8.5763	95.3870	9.1147	1155	1345	10.3059	8.0973	21.5444	1.8763	NO_2ss(79)
16	1321	-	1090	1326	1.4270	1.0006	43.7317	0.3530	1041	1319	6.2542	3.9959	75.1422	0.2461	NO_2ss(76)
17	1303	-	1025	1309	11.1274	6.8881	34.372	1.2110	985	1300	1.4675	0.8394	29.5744	0.5995	νCF(73)
18		1275	977	1275	1.4510	0.8172	37.8045	0.2701	868	1271	1.3202	0.5857	29.2132	0.2985	νCF(75)
19	1214	-	919	1216	12.6910	6.3191	0.8929	3.0248	833	1210	7.1102	2.9054	0.3035	3.3918	R trigd(74)
20	1172	1172	893	1174	8.0407	3.7781	24.1348	1.8532	792	1168	12.9839	4.7994	11.0099	22.3977	R symd(76)
21	1146	-	868	1149	9.3866	4.1728	12.6632	1.2391	768	1142	12.7723	4.4359	0.5338	1.2002	R asymd(73)
22		962	849	961	14.3200	6.0904	1.0305	41.1312	744	960	7.8037	2.5481	1.8059	11.0357	NO_2sciss(70)
23	915	910	777	919	4.6232	1.6450	4.5808	5.3663	730	917	6.5675	2.0635	14.6531	1.4164	NO_2sciss(69)

24	875	-	770	881	11.1685	3.9019	37.1315	0.2401	702	870	8.5761	2.4877	47.0157	0.8254	NO_2 rock(72)
25	840	-	755	842	6.7997	2.2876	1.3170	7.7733	641	845	6.6610	1.6225	2.1228	1.4507	NO_2 rock(69)
26	745	742	708	749	9.8694	2.9150	105.6784	2.2503	634	743	7.1119	1.6866	26.2337	0.6954	b CN(71)
27	-	732	666	732	6.0026	1.5710	0.1576	0.4944	598	730	9.8804	2.0804	23.5520	1.9022	b CN(68)
28	739	-	627	732	10.0626	2.3360	78.1847	2.9405	588	728	10.1548	2.0671	0.0613	1.8828	ω CH(69)
29	-	710	561	698	4.2803	0.7958	0.5096	1.7525	499	696	5.0408	0.7395	0.5367	3.9421	ω CH(70)
30	700	-	509	705	12.0917	1.8492	0.7854	0.0031	453	705	5.1272	0.6207	1.3066	1.9466	b CF(67)
31	666	-	506	664	7.6960	1.1645	8.5587	2.8479	428	660	12.7667	1.3759	1.2995	0.2143	b CF(65)
32	641	-	407	645	13.9220	1.3623	0.1191	3.2843	358	642	13.5845	1.0258	2.6359	6.5678	t Rtrigd(64)
33	622	-	405	621	14.4329	1.4015	3.2676	3.9974	337	620	13.6628	0.9119	0.0680	1.4508	t R symd(63)
34	599	-	355	605	13.9906	1.0400	0.0009	1.2102	304	602	14.0985	0.7668	0.3549	1.5822	t R asymd(67)
35	-	463	345	467	16.0611	1.1267	1.4166	2.9010	301	460	16.8941	0.9024	3.7162	1.5527	ω CN(65)
36	-	380	322	386	7.1102	0.4369	1.9688	1.5989	240	378	7.3789	0.2513	1.1697	1.7066	ω CN(64)
37	-	350	301	348	15.3091	0.8197	0.8101	0.5305	230	345	14.5479	0.4534	1.1672	0.7082	ω CF(62)
38	-	335	276	337	15.79350	0.7134	0.0463	0.1302	204	331	14.3853	0.2024	3.3161	0.5756	ω CF(61)
39	-	250	270	249	14.3871	0.6225	0.1813	5.2015	195	246	9.6551	0.0992	11.1914	0.8575	NO_2 twist(59)
40.	-	240	242	241	9.9416	0.3435	7.8464	1.0215	180	241	17.4043	0.663	0.0017	0.1598	NO_2 twist(60)
41.	-	150	209	157	11.6161	0.3001	8.2445	0.2776	168	152	15.3662	0.0196	0.7406	4.5455	NO_2 wag(58)
42.	-	140	150	139	17.2314	0.2311	0.0017	0.1579	147	135	15.9833	0.0167	0.1352	0.2323	NO_2 wag(57)

Abbreviations: ν - stretching; as - asymmetric stretching; ss - symmetric stretching; b - in-plane-bending; ω - out-of-plane bending; t - torsion.

Table 8: The observed (FT-IR and FT-Raman) and calculated (Unscaled and Scaled) frequencies (cm^{-1}), IR intensity (Km mol^{-1}), Raman activity (A^4 amu^{-1}) and probable assignments (characterized by TED) of 1-chloro-2,4-dinitrobenzene using B3LYP/6-311++G(d,p) and HF/6-311++G(d,p) calculations.

S. No.	Observed frequency (cm^{-1})		HF/6-311++G(d,p)						B3LYP/6-311++G(d,p)						Assignment % of TED
	FT-IR	FT-Raman	Calculated frequencies (cm^{-1})		Reduced Mass	Force Constants	IR Intensity	Raman Activity	Calculated frequencies (cm^{-1})		Reduced Mass	Force Constants	IR Intensity	Raman Activity	
			Unscaled	Scaled					Unscaled	Scaled					
1	3108	-	3464	3106	1.0912	7.3252	27.9670	32.9386	3410	3103	1.0898	7.4698	27.1966	33.0750	vCH(99)
2	3096	3098	3440	3094	1.0938	7.2569	7.5742	85.3899	3388	3093	1.0929	7.3919	7.1516	75.9222	vCH(97)
3	3027	-	3416	3026	1.0913	7.1415	0.7165	60.4505	3366	3022	1.0898	7.2781	0.6897	52.9638	vCH(96)
4	1612	-	1178	1616	9.4495	15.9508	27.8152	28.1464	1685	1609	8.8447	14.8051	21.2315	32.9546	vCC(94)
5	1600	-	1757	1607	7.9867	13.1139	84.3883	128.205	1668	1601	7.9905	13.1117	41.5771	64.5037	vCC(95)
6	-	1593	1651	1601	4.0330	5.5147	104.881	24.7914	1559	1595	7.9639	11.4097	118.8468	17.5983	NO_2ass(92)
7	1535	1538	1559	1534	9.2022	12.1485	174.404	39.4807	1549	1534	12.9155	18.2814	88.2001	12.9365	NO_2ass(96)
8	-	1478	1449	1481	7.3753	9.4991	99.2789	4.9129	1456	1474	3.2191	4.4189	8.3196	0.4106	vCC(89)
9	1467	-	1416	1469	5.9028	7.1557	77.3477	7.8121	1449	1461	4.5329	5.6143	1.5649	2.8434	vCC(88)
10	-	1392	1409	1399	10.1886	12.2532	59.5589	14.8916	1431	1390	10.7010	12.9187	15.9593	7.4385	vCC(87)
11	-	1362	1368	1368	10.8003	11.4397	284.962	408.576	1317	1360	4.9459	5.0568	132.5840	187.8840	NO_{2ss}(85)
12	1350	-	1338	1355	11.0458	11.2163	279.889	80.625	1295	1347	2.2512	2.2249	49.8726	57.4712	NO_{2ss}(83)
13	1298	1300	1307	1309	1.3925	1.3023	32.7033	6.2231	1287	1300	4.1151	4.0222	210.3238	29.5443	vCC(82)
14	-	1255	1268	1267	7.6217	6.4390	3.1659	30.7732	1215	1258	7.1053	6.1887	2.7966	17.5455	vCN(80)
15	1242	-	1242	1249	1.2707	0.9867	7.0566	1.5431	1179	1242	1.3662	1.1208	6.0470	1.7345	vCN(81)
16	1157	1160	1234	1167	1.4441	1.0421	14.1421	0.1567	1128	1163	1.6348	1.2261	15.8996	0.7270	bCH(79)
17	1140	1144	1228	1139	7.2274	4.7349	69.4844	23.1361	1084	1132	4.6851	3.2463	61.8113	6.2515	bCH(76)
18	1103	1100	1208	1114	1.3769	0.7423	0.1649	0.0413	1060	1114	1.8048	1.1957	14.0339	1.7762	bCH(74)
19	1048	1045	1154	1055	6.8981	3.6027	20.9364	2.7369	1037	1048	1.4303	0.9069	8.2493	0.6649	Rtrigd(73)
20	916	915	1039	923	1.5072	0.7218	14.9277	0.3777	924	917	8.1315	4.0966	33.5087	4.4165	Rsymd(70)
21	903	900	954	916	13.4290	5.5845	18.2162	26.4916	871	906	1.7523	0.7839	30.0144	2.4426	Rasymd(74)
22	861	-	911	868	1.7971	0.6797	16.5784	0.3724	811	862	12.7719	4.9573	28.6869	7.8098	ωCH(69)
23	845	843	844	848	5.2261	1.8033	0.6536	1.0663	793	841	2.4004	0.8897	2.6650	0.4861	ωCH(68)

24	836	-	812	847	10.5344	3.4919	19.5171	0.7851	739	839	10.3229	3.3271	31.4193	1.4256	ωCH(66)
25	749	750	782	758	5.9225	1.8045	29.4409	0.6242	714	752	4.7952	1.4403	8.0402	2.6140	νCCl(72)
26	-	742	745	747	7.2500	1.9869	11.6443	3.9505	696	741	7.6827	2.1976	12.2078	3.8878	No_2sciss(70)
27	734	-	732	738	5.1886	1.2715	5.3716	1.2069	640	731	7.1734	1.7354	26.7877	1.7227	No_2sciss(69)
28	694	-	655	695	5.8655	1.2642	13.4356	0.5097	604	688	7.2195	1.5661	26.5137	1.4231	bCN(69)
29	-	688	600	681	8.9248	1.5613	8.9758	3.6404	530	681	6.7205	1.1131	11.5550	1.4506	bCN(68)
30	-	670	558	667	8.3068	1.2902	15.0820	2.3140	515	663	6.5273	1.0209	6.5892	2.5492	No_2wag(66)
31	662	-	540	658	4.3652	0.5613	6.9270	0.7008	488	653	4.9235	0.6932	7.6474	2.5409	No_2wag(65)
32	605	-	508	604	3.4102	0.3366	2.7962	0.2700	445	599	3.6025	0.4208	0.3153	0.3777	tR_{trigd}(64)
33	-	550	391	545	9.2894	0.7672	0.7747	3.9485	362	537	12.7610	0.9893	0.7685	5.7824	tR_{symd}(65)
34	536	-	361	531	8.7409	0.6516	0.9588	1.2629	327	526	18.3271	1.1573	0.1667	4.0414	tRasymd(67)
35	-	522	341	512	18.9838	1.0805	0.8614	2.9218	306	509	9.6804	0.5374	1.2055	0.5402	No_{2rock}(65)
36	485	485	337	478	7.5251	0.3423	0.5185	0.7279	270	475	8.6895	0.3759	0.7868	0.5346	No_2rock(66)
37	-	372	240	367	19.9483	0.6348	0.1154	0.7500	212	361	19.4426	0.5165	0.4760	1.0857	bCCl(68)
38	-	325	190	325	13.6088	0.2697	3.5082	0.1064	185	317	9.9654	0.0885	3.9307	0.6853	ωCN(64)
39	-	285	180	279	15.8013	0.1700	0.1331	1.0396	176	272	6.8858	0.0402	1.9004	2.5086	ωCCL(63)
40	-	214	104	207	14.5279	0.1380	0.0950	1.3746	169	201	9.5259	0.0167	3.3861	1.1340	ωCCL(65)
41	-	165	99	162	8.2353	0.0679	5.6417	0.7035	91	157	15.5549	0.2249	0.3805	1.0527	NO_{2twist}(63)
42	-	102	88	99	5.8260	0.0130	0.9182	1.4310	84	93	16.0348	0.2745	0.0786	1.3564	NO_{2twist}(62)

Abbreviations: ν - stretching; as - asymmetric stretching; ss - symmetric stretching; b - in-plane-bending; ω - out-of-plane bending; t - torsion.

Table 9: Nonlinear optical properties of 1,5-difluoro-2,4-dinitrobenzene and 1-chloro-2,4–dinitrobenzene based on B3LYP/6-311++G(d,p) method.

NLO behavior	Values	
	1,5-difluoro-2,4-dinitrobenzene	1-chloro-2,4–dinitrobenzene
Dipole moment (μ)	3.1460 Debye	4.2227 Debye
Mean polarizability (α)	0.90654×10^{-30} e.s.u	2.1593×10^{-30} e.s.u
Anisotropy of the polarizability (Δα)	2.2373×10^{-30} e.s.u	7.714×10^{-30} e.s.u
First hyperpolarizability (β)	4.7869×10^{-30} e.s.u	1.398×10^{-30} e.s.u

Table 10: HOMO-LUMO energy and other related properties of 1,5-difluoro-2,4-dinitrobenzene and 1-chloro-2,4-dinitrobenzene in a.u. based on B3LYP/6-311++G(d,p) method.

Parameters	1,5-difluoro-2,4-dinitrobenzene	1-chloro-2,4-dinitrobenzene
HOMO	-0.29193	-0.31295
LUMO	-0.22155	-0.17115
The global hardness (η)	0.03519	0.05753
Electronic chemical potential (μ)	-0.25674	-0.0709
Electrophilicity index (ω)	0.93656	0.04368
Ionization energy (I)	0.29193	0.31295
Electron affinity (A)	0.22155	0.17115

Table 11: Second order perturbation theory of Fock matrix in NBO basis of 1,5-difluoro-2,4-dinitrobenzene based on B3LYP/6-311++G(d,p) method.

Donor NBO (i)	Acceptor NBO (j)	Occupancy	E(2) jK/mol	E(j) – E(i) a.u.	F(i, j) a.u.
σ (C_1-C_2)	σ*(C_2-C_3)	0.98915	7.6149	1.28	0.061
Π (C_1-C_2)	Π* (C_5-C_6)	0.81696	35.02	0.29	0.062
Π (C_1-C_2)	Π*(N_8-O_9)	0.82303	42.4676	0.16	0.055
σ (C_2-C_3)	σ*(C_1-F_7)	0.99695	8.4517	0.94	0.055
σ (C_2-C_2)	σ*(C_4-N_{12})	0.98895	7.4475	1.01	0.054
σ (C_3-C_4)	σ*(C_5-F_{15})	0.99692	8.4517	0.94	0.055
Π (C_3-C_4)	Π*(N_{12}-O_{13})	0.81616	50.124	0.15	0.057
σ (C_3-H_{11})	σ*(C_4-C_5)	0.98898	8.6609	1.04	0.058
σ (C_4-C_5)	σ*(C_3-C_4)	0.98910	7.573	1.28	0.061
Π (C_5-C_6)	Π*(C_1-C_2)	0.82348	53.179	0.27	0.076
σ (C_6-H_{16})	σ*(C_1-C_2)	0.98911	8.2006	1.04	0.057
Π (N_8-O_9)	Π*(C_1-C_2)	0.99105	8.7446	0.42	0.042
Π (N_8-O_9)	Π*(N_8-O_9)	0.98103	16.652	0.30	0.052
Π (N_{12}-O_{13})	Π*(N_{12}-O_{13})	0.99098	18.326	0.29	0.055
n_3 F_7	Π*(C_1-C_2)	0.95669	42.007	0.38	0.086
n_2 O_9	σ*(N_8-O_{10})	0.95415	38.702	0.61	0.095
n_2 O_{10}	σ*(N_8-O_9)	0.99992	36.484	0.61	0.093
n_3 O_{10}	Π*(N_8-O_9)	0.71277	339.677	0.12	0.0127
n_2 O_{13}	σ*(N_{12}-O_{14})	0.95415	34.225	0.62	0.094
n_3 O_{14}	Π*(N_{12}-O_{13})	0.95415	372.125	0.12	0.130
n_3 F_{15}	Π*(C_5-C_6)	0.95669	40.125	0.39	0.083

Table 12: Second order perturbation theory analysis of Fock matrix in NBO basis of 1-chloro-2,4-dinitrobenzene based on B3LYP/6-311++G(d,p) method.

Donor NBO (i)	Acceptor NBO (j)	Occupancy	E(2) jK/mol	E(j) – E(i) a.u.	F(i, j) a.u.
$\pi^*(C_1-C_6)$	$\pi^*(C_2-C_3)$	0.36967	232.11	0.01	0.076
$\pi^*(C_1-C_6)$	$\pi^*(C_4-C_5)$	0.36967	247.93	0.01	0.086
$n_3\ O_{14}$	$\pi^*(N_7-O_9)$	1.42862	157.78	0.15	0.139
$\pi(C_4-C_5)$	$\pi^*(N_{12}-O_{13})$	1.62320	26.87	0.15	0.061
$\pi(C_4-C_5)$	$\pi^*(C_2-C_3)$	1.62320	24.70	0.28	0.075
$\pi(C_1-C_6)$	$\pi^*(C_4-C_5)$	1.63561	21.98	0.29	0.071
$\pi(C_2-C_3)$	$\pi^*(C_1-C_6)$	1.65033	21.78	0.28	0.070
$n_2\ O_{13}$	$\sigma^*(N_{12}-O_{14})$	1.89546	19.45	0.71	0.106
$n_2\ O_9$	$\sigma^*(N_7-O_{10})$	1.89235	19.42	0.70	0.105
$n_2\ O_{14}$	$\sigma^*(N_{12}-O_{13})$	1.89640	19.28	0.71	0.106
$\pi(C_4-C_5)$	$\pi^*(C_1-C_6)$	1.62320	19.00	0.27	0.064
$n_2\ O_{10}$	$\pi^*(N_7-O_9)$	1.89318	18.74	0.71	0.104
$\pi(C_1-C_6)$	$\pi^*(C_2-C_3)$	1.63561	17.91	0.29	0.064
$\pi(C_2-C_3)$	$\pi^*(N_7-O_9)$	1.65033	17.53	0.17	0.051
$\pi(C_2-C_3)$	$\pi^*(C_4-C_5)$	1.65033	16.80	0.29	0.063
$\pi^*(N_{12}-O_{13})$	$\pi^*(C_4-C_5)$	0.61965	15.57	0.13	0.058
$n_3\ Cl_8$	$\pi^*(C_1-C_6)$	1.89873	14.90	0.31	0.065
$n_2\ O_9$	$\sigma^*(C_2-N_7)$	1.89235	13.07	0.55	0.076
$n_2\ O_{10}$	$\sigma^*(C_2-N_7)$	1.89318	12.70	0.55	0.075
$n_2\ O_{13}$	$\sigma^*(C_4-N_{12})$	1.89546	12.48	0.56	0.075
$\pi(N_7-O_9)$	$n_3\ O_{10}$	1.98586	12.40	0.19	0.079
$\pi(N_{12}-O_{13})$	$n_3\ O_{14}$	1.98532	12.36	0.18	0.078
$n_2\ O_{14}$	$\sigma^*(C_4-N_{12})$	1.89640	12.35	0.56	0.074
$\pi^*(N_7-O_9)$	$\pi^*(C_2-C_3)$	0.59801	10.70	0.12	0.047
$\pi(N_{12}-O_{13})$	$\pi^*(N_{12}-O_{13})$	1.98532	7.38	0.32	0.052
$\pi(N_7-O_9)$	$\pi^*(N_7-O_9)$	1.98586	6.53	0.34	0.050
$n_1\ O_{14}$	$\sigma^*(C_4-N_{12})$	1.98071	4.20	1.07	0.061
$\pi(N_{12}-O_{13})$	$\pi^*(C_4-C_5)$	1.98532	4.19	0.45	0.043

Table 13: Theoretically computed zero point vibrational energy (kcal mol^{-1}), rotational constant (GHz), rotational temperature (kelvin), thermal energy (kcal mol^{-1}), molar capacity at constant volume (cal mol^{-1} kelvin^{-1}), entropy (cal mol^{-1} kelvin^{-1}), dipole moment (Debyes) and vibrational temperature (kelvin) by B3LYP/6-311++G(d,p) method for 1,5-difluoro-2,4-dinitrobenzene and 1-chloro-2,4-dinitrobenzene.

Parameter	1,5-difluoro-2,4-dinitrobenzene	1-chloro-2,4-dinitrobenzene
Zero-point vibrational energy	54.19002	56.04403
Rotational constant	1.14935 0.48797 0.35135	1.47626 0.42048 0.35207
Rotational temperatures	0.05516 0.02342 0.01686	0.07085 0.02018 0.01690
Energy		
Total	61.325	62.580
Translation	0.889	0.889
Rotational	0.889	0.889
Vibrational	59.547	60.802
Molar capacity at constant volume		
Total	41.037	40.994
Translational	2.981	2.981
Rotational	2.981	2.981
Vibrational	35.076	35.032
Entropy		
Total	108.108	99.742
Translational	41.843	41.814
Rotational	31.767	31.665
Vibrational	34.498	26.264

Table 14: The charge distribution of 1,5-difluoro-2,4-dinitrobenzene and 1-chloro-2,4-dinitrobenzene based on B3LYP/6-311++G(d,p) method.

Atoms	Atomic Charges (Mulliken)	
	1,5-difluoro-2,4-dinitrobenzene	1-chloro-2,4–dinitrobenzene
C_1	0.121156	-0.290636
C_2	0.286609	0.329510
C_3	-0.155071	-0.138965
C_4	0.286505	0.270593
C_5	0.121195	-0.155825
C_6	-0.089952	-0.192511
Cl_7	-0.265961	0.252589
N_8	-0.393093	0.175381
O_9	0.046876	-0.346428
O_{10}	0.020920	-0.369132
H_{11}	0.328572	0.376587
N_{12}	-0.393047	0.179724
O_{13}	0.020891	-0.365679
O_{14}	0.046898	-0.372704
H_{15}	-0.265977	0.336817
H_{16}	0.283480	0.310678

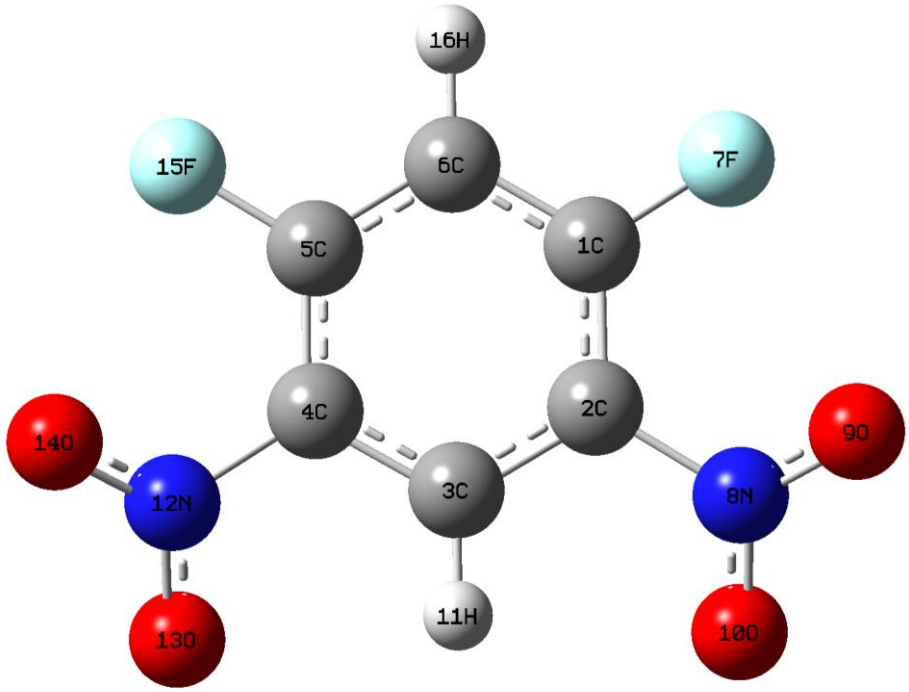

Fig. 1: Molecular Structure of 1,5-difluoro-2,4-dinitrobenzene

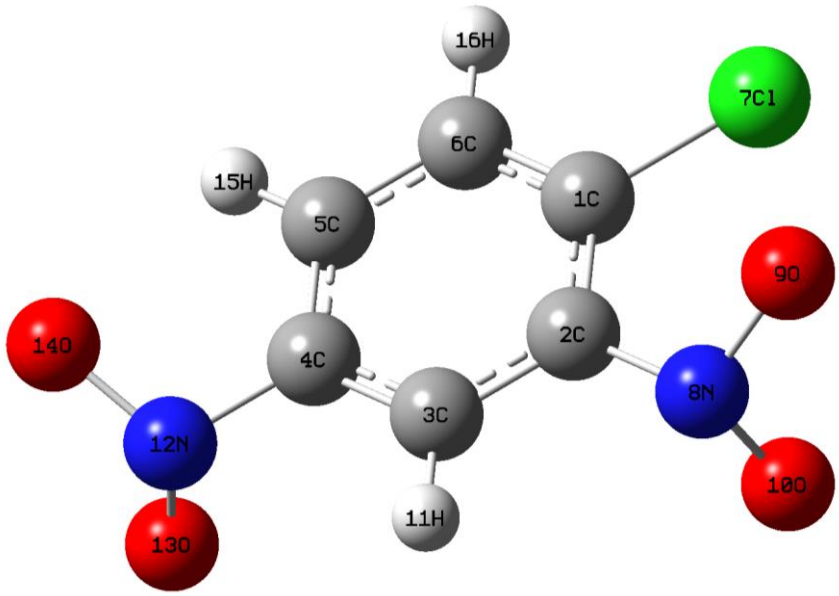

Fig. 2: Molecular Structure of 1-chloro-2,4-dinitrobenzene

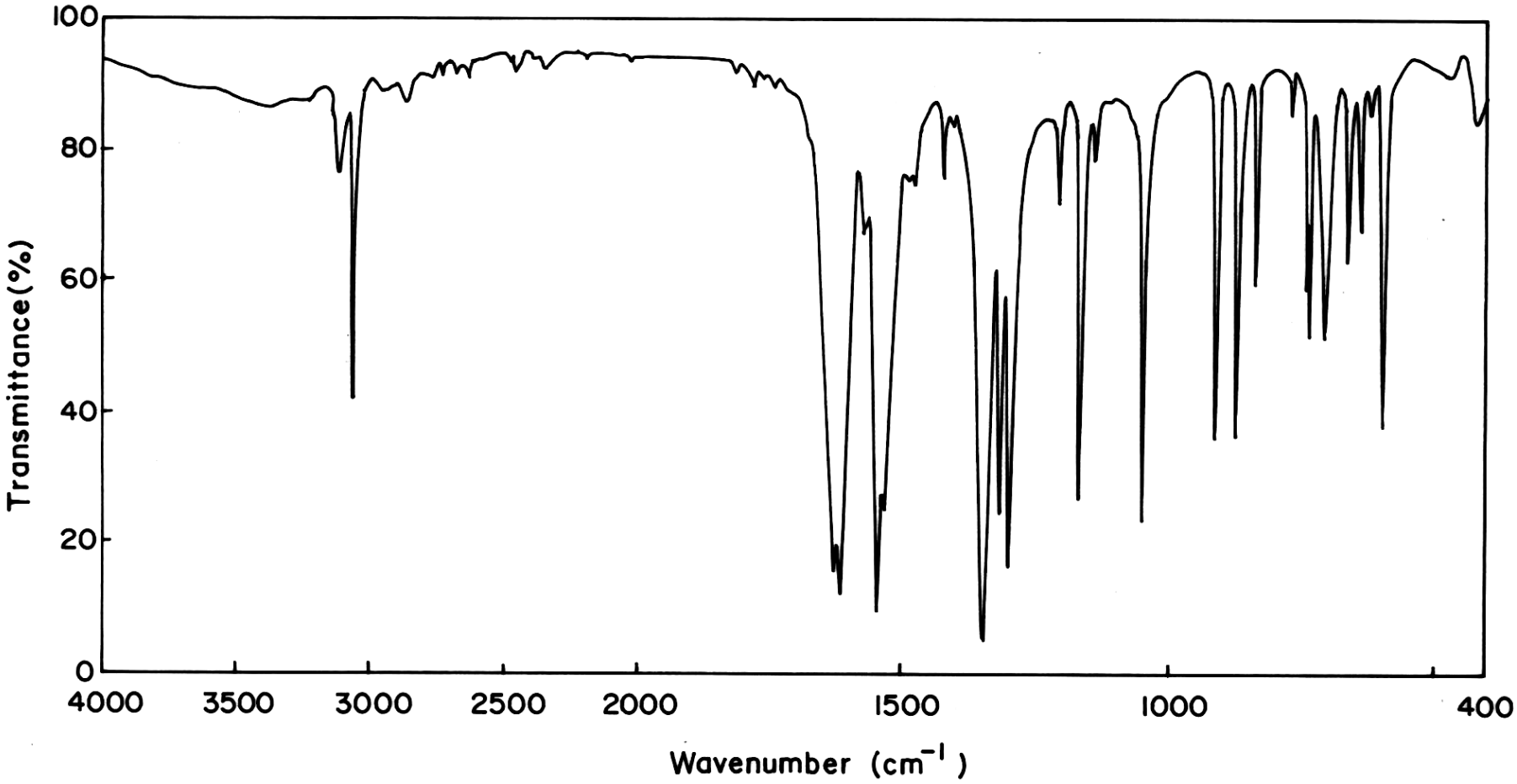

Fig. 3: FT-IR spectrum of 1,5-difluoro-2,4-dinitrobenzene

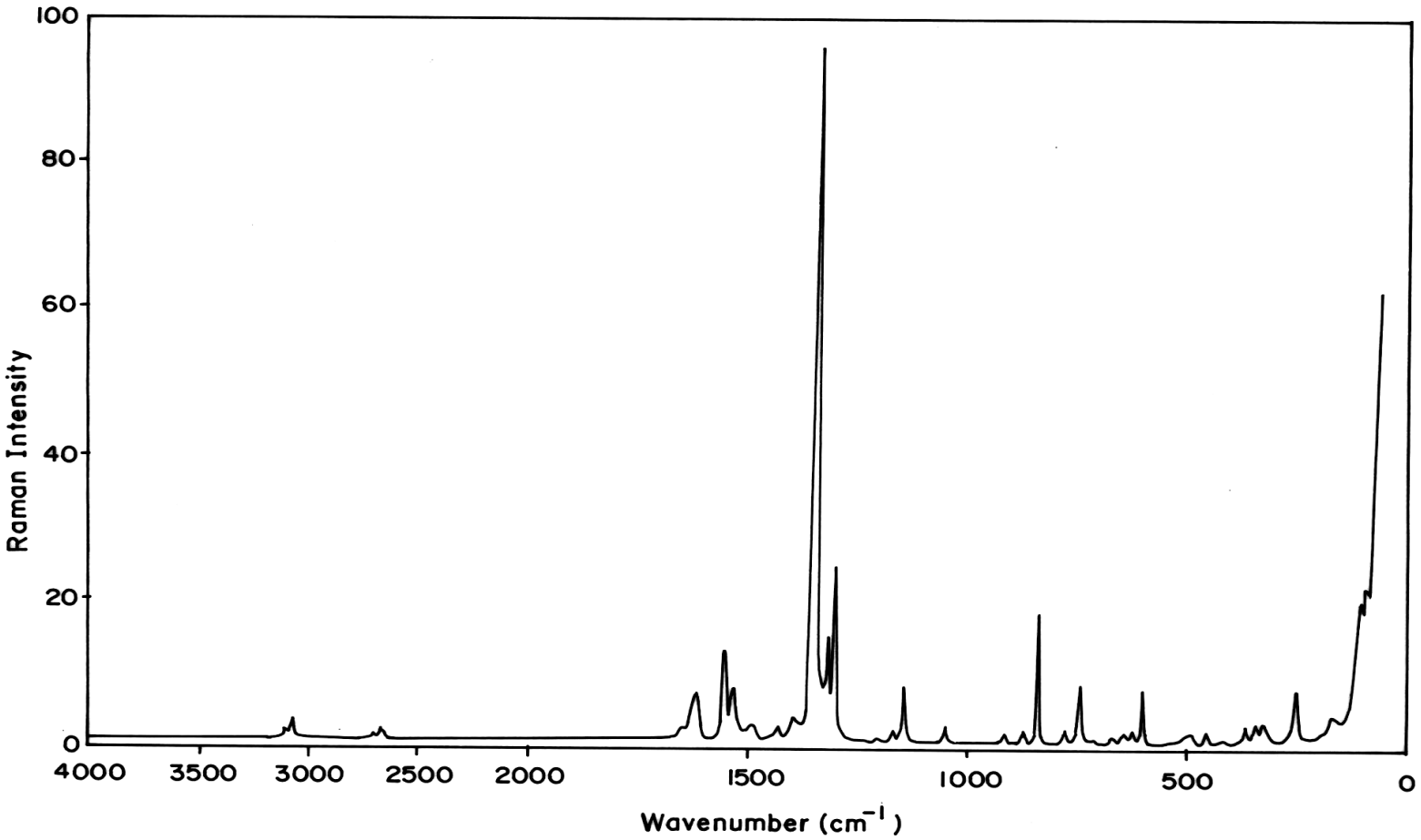

Fig. 4: FT-Raman spectrum of 1,5-difluoro-2,4-dinitrobenzene

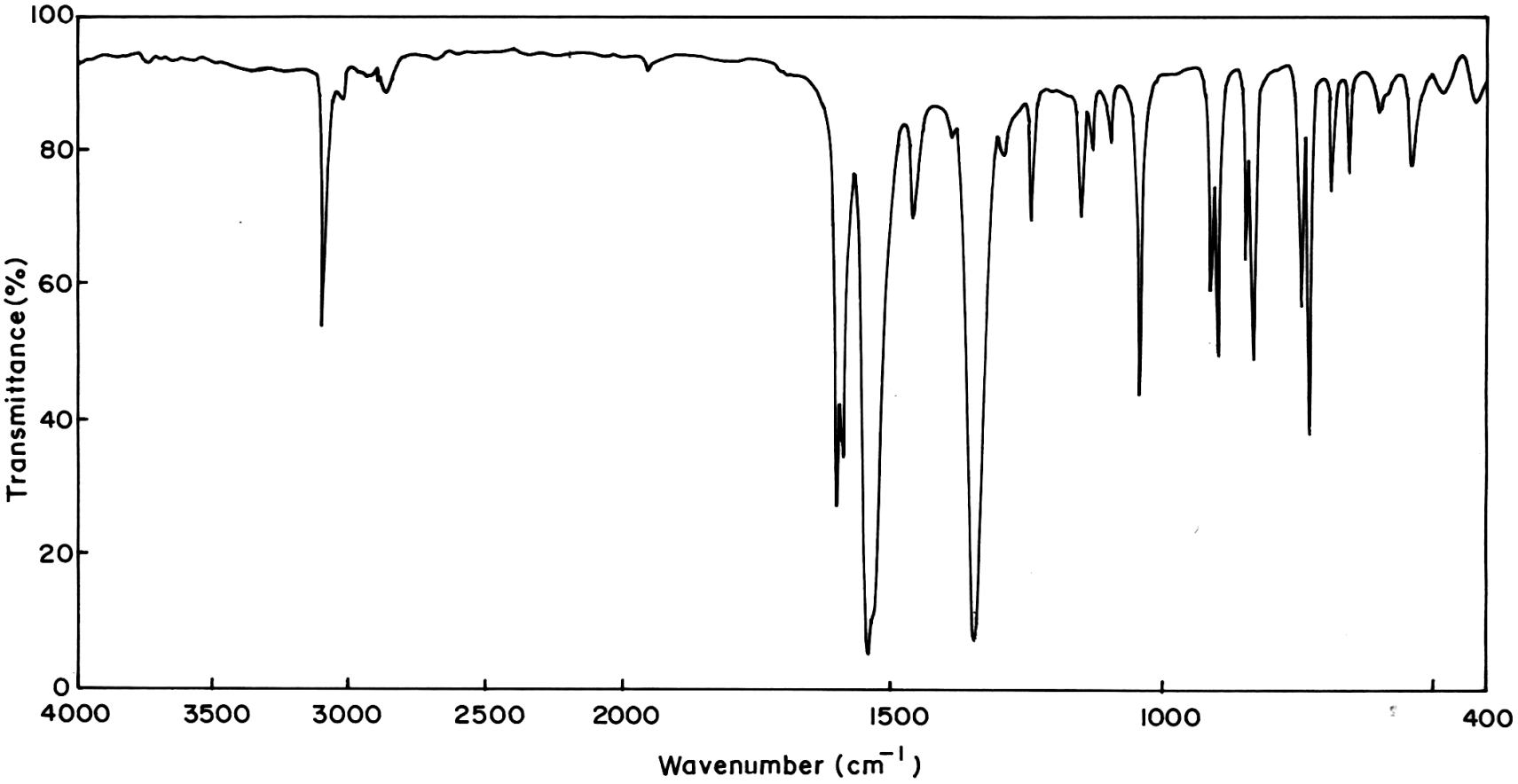

Fig. 5: FT-IR spectrum of 1-chloro-2,4-dinitrobenzene

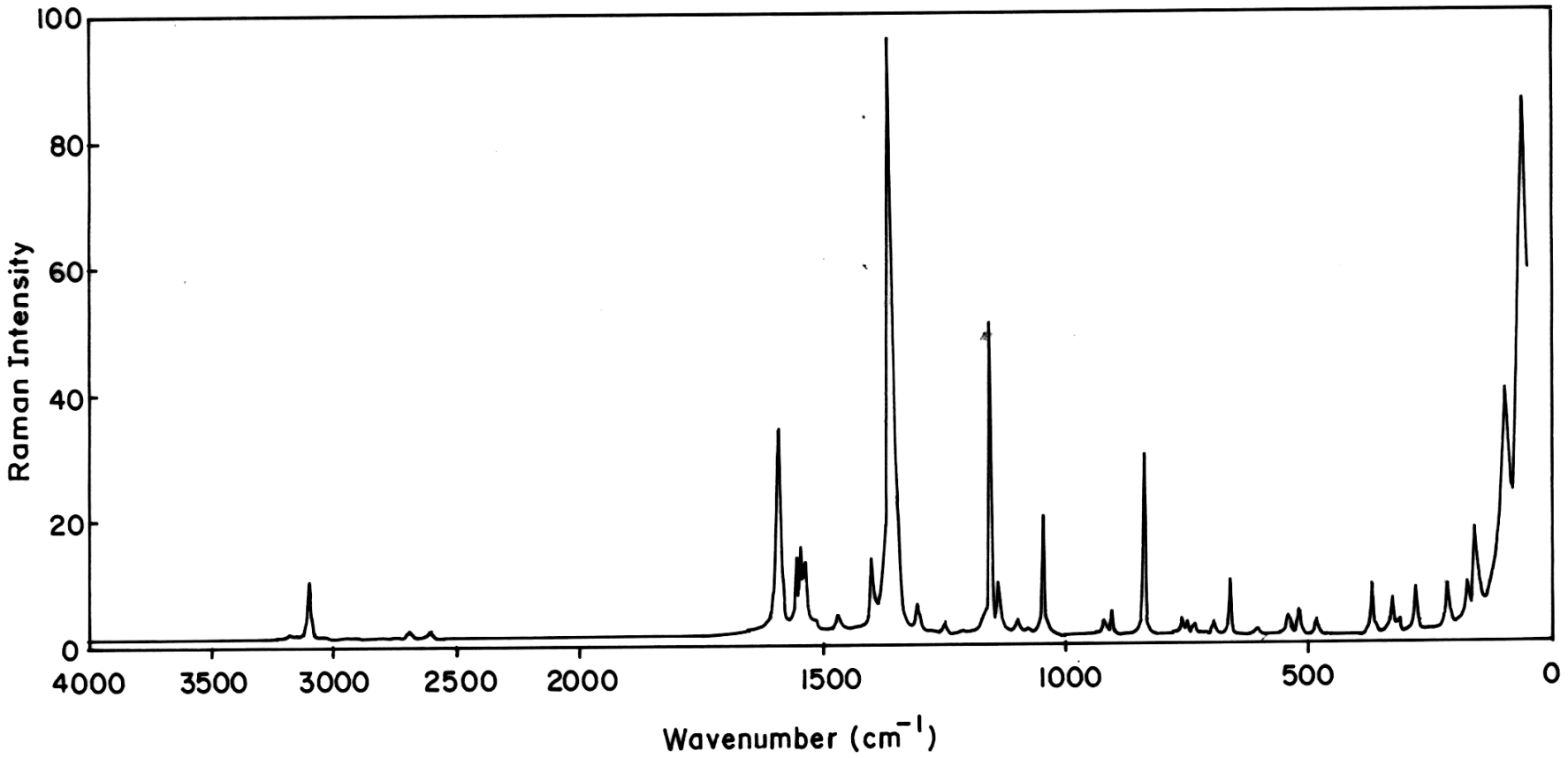

Fig. 6: FT-Raman spectrum of 1-chloro-2,4-dinitrobenzene

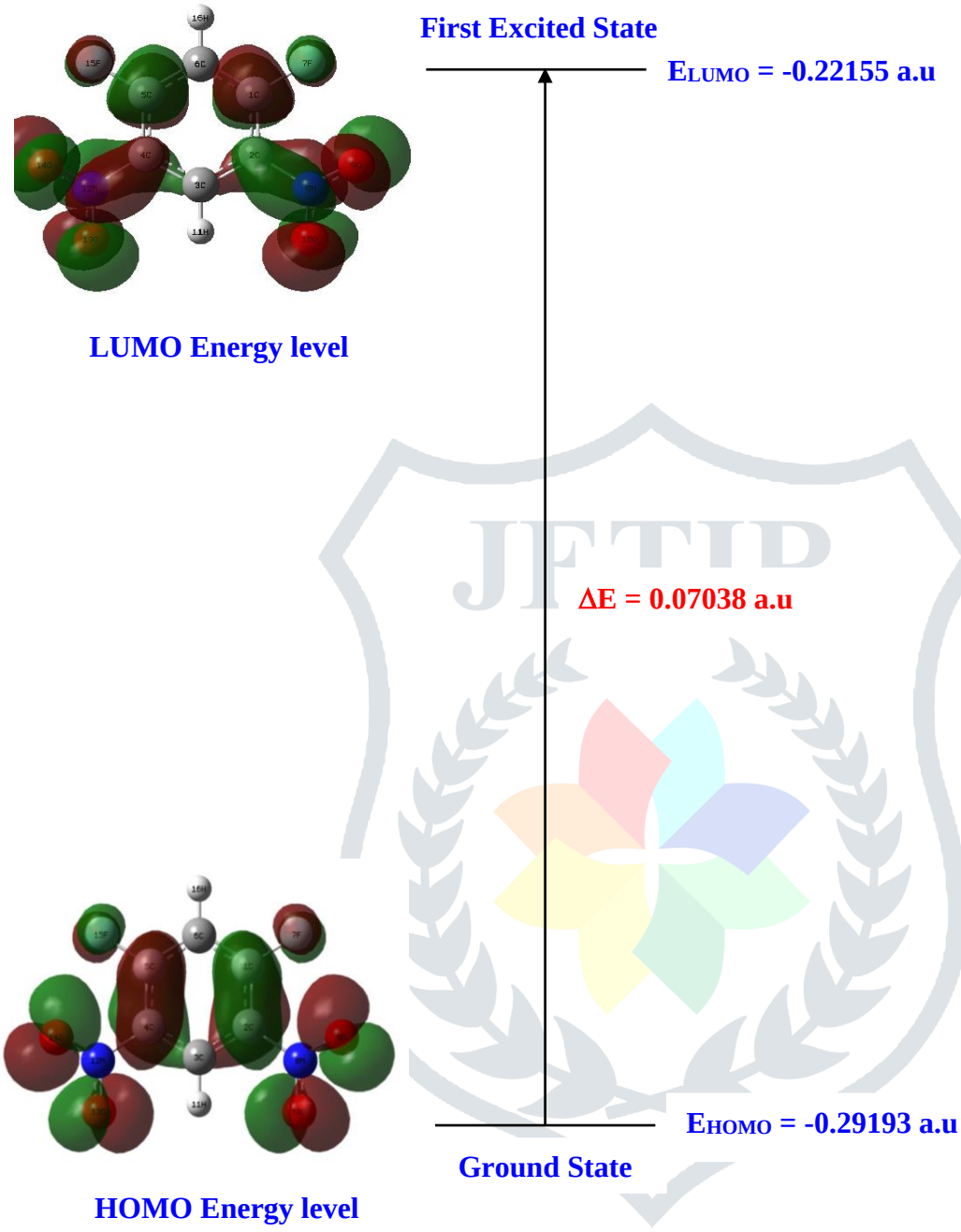

Fig. 7: The Frontier orbitals of 1,5-difluoro-2,4-dinitrobenzene

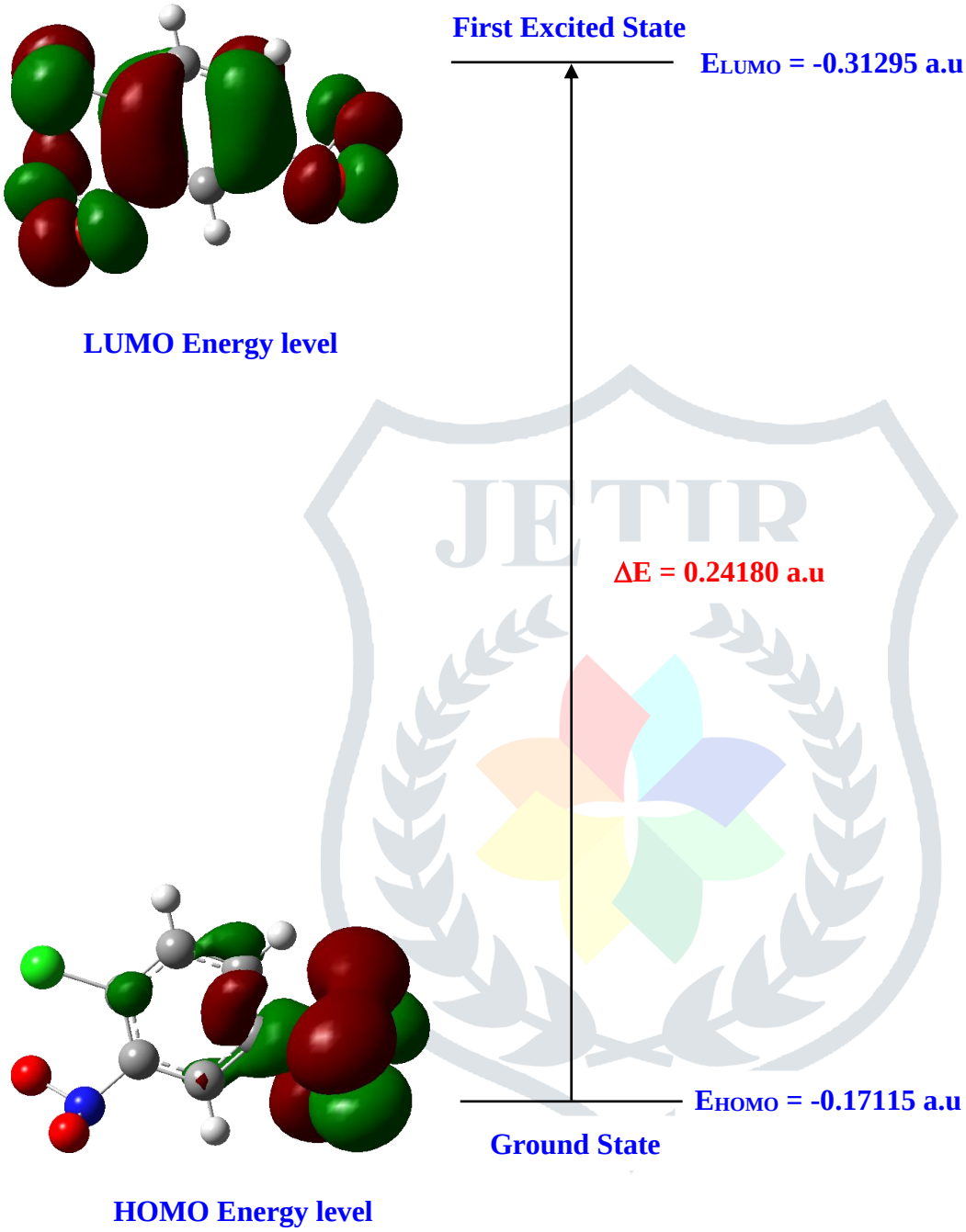

Fig. 8: The Frontier orbitals of 1-chloro-2,4-dinitrobenzene

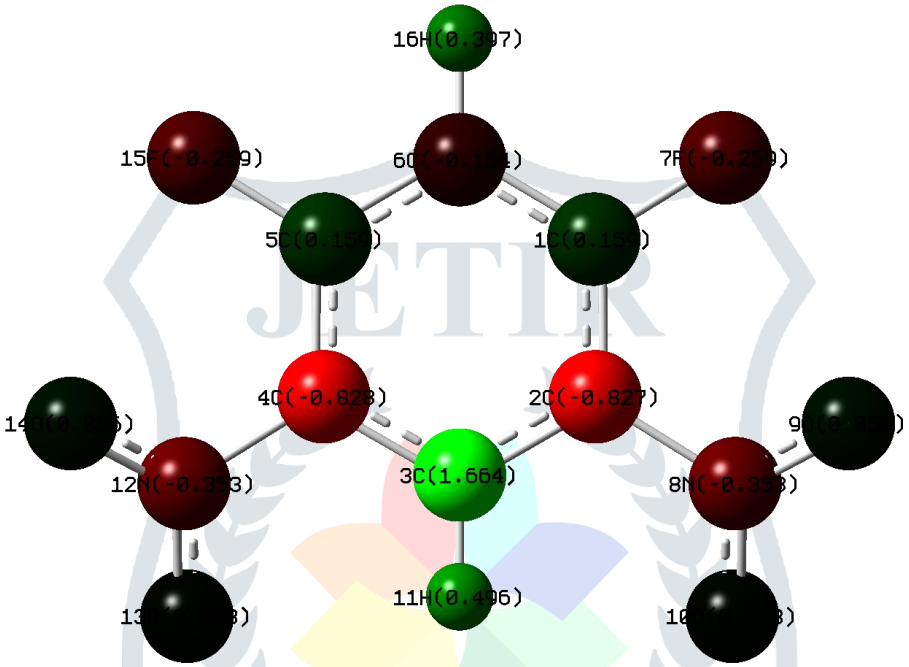

Fig. 9: Mulliken Plot of 1,5-difluoro-2,4-dinitrobenzene

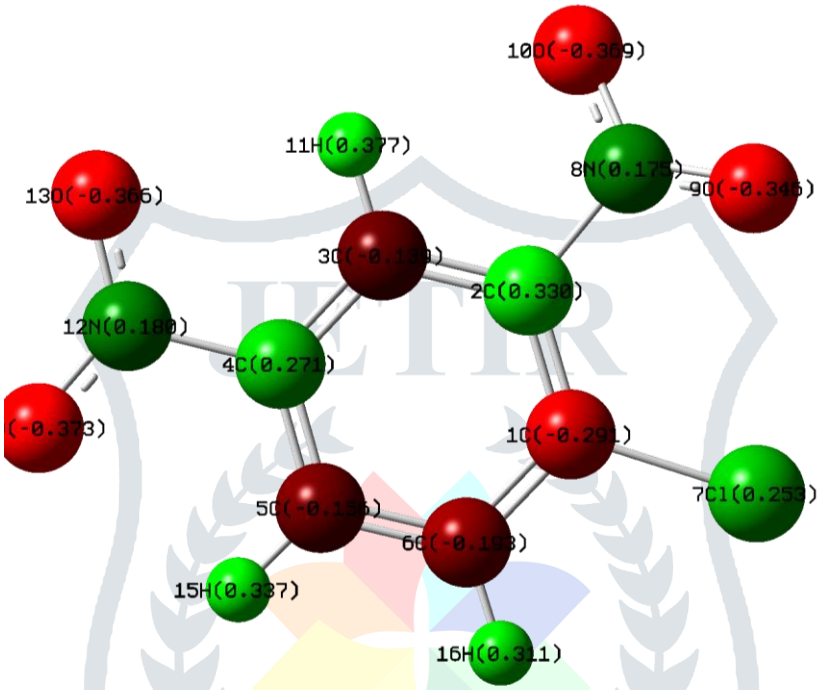

Fig. 10: Mulliken Plot of 1-chloro-2,4-dinitrobenzene